Double ionization of water molecules induced by swift protons

A. C. Tavares
Departamento de Física, Pontifícia Universidade Católica do Rio de Janeiro, Caixa Postal 38071, 22452-970 Rio de Janeiro, Rio de Janeiro, Brazil

H. Luna,* W. Wolff, and E. C. Montenegro
Departamento de Física, Universidade Federal do Rio de Janeiro, Caixa Postal 68528, 21945-970 Rio de Janeiro, Rio de Janeiro, Brazil

(Received 2 June 2015; published 29 September 2015)

Experimental cross sections for single and double ionization of H_2O by swift H^+ with energy ranging from 0.3 to 2.0 MeV are reported. In this energy range the ionization is the dominant collision process and charge transfer reactions can be disregarded. A multihit coincidence technique is used to measure the $H^+ + OH^+$ and $H^+ + O^+$ fragmentation channels. Single- and double-hit differential measurements together with a semiempirical calculation allow separating quantitatively the prompt and Auger-like decay contributions to fragmentation following a vacancy in the $2a_1$ molecular orbital. Concerning the double-ionization channel, it is found that for lower energies the mechanism of a sequential double-electron removal, known as TS2, dominates. For energies above above 750 keV/u ionization resulting from a single vacancy followed by an Auger like deexcitation takes over the TS2, becoming the main contribution to the double-ionization cross section. Our results are compared to the electron-impact data within the same velocity range and also with theoretical calculations available in the literature.

DOI: 10.1103/PhysRevA.92.032714 PACS number(s): 34.50.Fa, 52.20.Hv, 82.30.Fi

I. INTRODUCTION

The ionization of molecules by fast-particle impact usually results in their fragmentation, producing highly reactive ionic radicals that strongly affect the surrounding environment with profound implications in areas such as the treatment of tumors [1–3] or the evolution of planetary atmospheres [4,5]. Swift protons can remove essentially any electron from a molecule, from the outermost to the innermost molecular levels. The removal of a particular electron results in a new electronic configuration and the system can be stabilized either as the parent molecule ion or as fragments by dissociating into one or more ionic species. In multielectronic molecules a number of final electronic states are associated with each of the fragment ions produced and it is a major challenge to predict how a certain molecule will dissociate from the knowledge of the distribution of primary vacancies produced by the projectile [6]. Thus, the relaxation phase and fragmentation that follow the projectile impact need to be investigated experimentally since there is no theoretical model available to properly quantify the proportions to which the various fragments are formed [7].

The removal of two or more electrons not only produces a larger number of ionic species but it can also open the pathway for the production of species not accessible when a single vacancy occurs in the ionization process. There are two main independent mechanisms of removing two electrons from a molecule: two successive impacts by the projectile on two target electrons, a mechanism known as TS2 in the literature [8–10], and by Auger decay, when the primary vacancy is in an inner valence orbital or in a more tightly bound state [11]. Separating and quantifying these two contributions is essential: first to verify accurately the collision dynamics calculations and second to establish properly the fragmentation pathways associated with the distribution of primary vacancies.

These two mechanisms have been studied in detail for collisions of fast protons and electrons with atomic and molecular targets [12–17]. It was shown that the constant ratio between double and single ionization, which is reached at high velocities, can be considered as a clear signature of a postcollisional Auger-like decay following a single vacancy produced by ionization [18,19]. The deviation from this constant ratio, for lower projectile velocities, has been assigned to the contribution of the TS2 mechanism. Because the maximum of the ionization cross section occurs at much lower velocities in the case of protons compared to electrons, the presence of TS2 can be seen much more clearly when the former are used as projectiles.

Several studies have been done to characterize the fragmentation of a doubly charged water molecule [20–24]. However, those studies have used low-energy or highly charged projectiles, in which the primary distribution of electron vacancy is not well known. A clear signature of the Auger contribution to the fragment ion production is advantageously obtained when swift singly charged projectiles are used.

The quantitative characterization of the fragmentation pathways is not straightforward, even in the region of higher velocities, when the TS2 mechanism can be disregarded. In the case of water, vacancies occur in the $2a_1$ inner valence molecular orbital and the Auger-like deexcitation channel is open but competes with a prompt single-vacancy fragmentation. The relative yields of these two alternatives are unknown. Indeed, previous works [7] strongly suggest that the production of O^+ in the high-velocity region originates from a primary single vacancy in the orbital $2a_1$. However, reports of the relative yields corresponding to the channels for $O^+ + 2H$ or H_2 (prompt) or $O^+ + H^+ + H$ (Auger-like deexcitation) are lacking.

*hluna@if.ufrj.br

In this work double-ionization cross sections of water leading to $H^+ + OH^+$ and $H^+ + O^+$ are measured using a multihit coincidence setup with the aim to separate the prompt contribution in the mass spectra and obtain a clean contribution from the Auger-like mechanism to these double-ionization channels. Further, from the velocity dependence of the ratios between double-ionization cross sections and the single-ionization channel (H_2O^+) for proton and electron impact [18,19], the contributions from both the Auger-like and the two-step process (TS2) to the total double-ionization cross section are also quantitatively obtained. The latter result is achieved by taking advantage of a model proposed by Montenegro and co-workers [7,25,26] to estimate the primary single-vacancy production by proton and electron impact.

Our results show that Auger decay contributes to at least 27%. This result indicates that prompt and Auger fragmentation processes occur in the same time scale, of the order of 10 fs. In addition, we found a clear preponderance of TS2 mechanism in the production of O^+ for low projectile energies, up to 300 keV/u. For higher energies, the deexcitation of a single vacancy in the $2a_1$ orbital becomes the dominant mechanism for the production of this ion.

Double ionization is responsible for the production of hydrated electron pairs and at the same time is the main precursor for the production of H_2 and O_2 in liquid water [27,28]. Knowledge of cross sections and the various fragmentation pathways of water by electron impact is essential to obtain realistic numerical simulation for modeling radiation damage in biological materials [29,30]. Therefore, for this purpose it is not sufficient to identify the ion fragments produced, such as OH^+ or O^+, but also how many electrons or, alternatively, how many neutral or charged fragments are released concurrently with the production of these ionic fragments. In this context, this work also provides necessary information to improve particle-track modeling in any liquid water environment.

II. EXPERIMENTAL PROCEDURE

The experimental setup used in this work has been described previously [31] and only the most important features will be given here. Briefly, a proton beam with energies ranging from 300 up to 2000 keV was obtained from a Pelletron accelerator facility at Federal University of Rio de Janeiro. The beam was mass-energy analyzed by a switching magnet and directed towards the projectile-target collision beam line.

The collision beam line is composed of two sets of collimation slits and three high vacuum chambers placed in tandem. The first one contains a gas cell target, used to measure total absolute cross sections. The second one contains an effusive jet target coupled to a time-of-flight mass spectrometer and it is used for ion-fragment partial-cross-section measurements. Finally, a third chamber is used to detect the main ion beam and its products generated from the interaction of either the gas cell or the effusive jet target. After the interaction of the proton beam with the effusive jet target, the ejected electrons and ionic fragments are extracted from the interaction region by means of a static electric field (700 V/cm), focused and accelerated into a field-free drift tube, and directed to the detectors. The time-of-flight spectra are determined by a multihit coincident setup composed of a fast time-to-digital converter. The proton-beam projectile is set as the starting pulse and the recoil ions products from the target are set as the sequential multihit stop signals (e.g., $H^+ + OH^+$), where the H^+ recoil provides the first stop and the OH^+ recoil provides the second stop, both in coincidence with the projectile as the start signal.

The projectile proton beam is detected using a solid-state detector that, provided the counting rate does not exceed 2.000 particles/s, has a 100% detection efficiency. The recoil ions are detected by a microchannel plate (MCP) detector in a chevron configuration. The MCP efficiency of a single fragment detection is not 100% and the procedure to obtain such efficiency (including the transmission through the electrodes grids) was discussed previously in Ref. [31] for the atomic target case. For a molecular target H_2O, on the other hand, multiple ionization leads to fragmentation and to the formation of multiple ionic fragments that will be detected sequentially (multihit detection). In this case, the efficiency related to the multihit detection conjugated with the Coulombic explosion effect (ion trajectory towards the detector) has to be taken into account carefully. The procedure adopted to determine the efficiency will be described in detail below.

For an atomic target or a single charged ion from a molecular target, the detection efficiency ϵ_q of a recoil ion of charge $q \geqslant 1$ can be approximated to be independent of the charge state q provided the recoil ion detector is working in the plateau regime (i.e., the detector operates in a mode where the efficiency is independent of the recoil ion mass and charge state and in this case to the recoil ion energy prior to the detection). Then an average efficiency $\bar{\epsilon}$ can be used to describe all recoil charge states [31]. For the water molecule, ionization of H_2O^{q+} with $q \geqslant 1$ leads to molecular fragmentation generating at least two singly charged fragments (e.g., $H^+ + OH^+$). Those ion-pair fragments, opposite to the single-ion case, accounts for the detection efficiency of two singly charged ions instead of the detection of only one doubly charged ion. The sequential detection of two singly charged ions can lead to a scenario where at least one of the ions produced, e.g., H^+ or OH^+, could not be detected. As a consequence, a doubly charged event ($q = 2$) can be measured as a singly charged event ($q = 1$) producing an artificial enhancement of single-ion channels such as $H_2O^+ \rightarrow H^+ + OH$ or $H + OH^+$. Therefore, it becomes mandatory to correct the measured production yields in order to obtain the true single-ion and ion-pair production yields.

The procedure used in this work to evaluate the true yields of single-ion and ion-pair fragment production follows a procedure similar to that presented in the work of Ben-Itzhak *et al.* [32]. First we define the single-ion detection efficiency ϵ_i, which depends only on the recoil ion detector (MCP) characteristic. The index i is used to take into account different ion masses and charge states.

Second, for the single-ion detection efficiencies ϵ_i an average efficiency $\bar{\epsilon}$ is used by assuming that the detection is independent of the recoil ion charge state (energy) and mass as discussed in Ref. [31]. This is achieved by monitoring the ionization of noble gases and increasing the voltage in the front grid of the MCP, up to the point where the ratios Ne^{2+}/Ne^+ and Ne^{3+}/Ne^+ become constant. For consistency, we compared the ratios Ne^{2+}/Ne^+, Xe^{2+}/Xe^+, and Ar^{2+}/Ar^+

for a 2-MeV proton ionization with the data available in the literature, obtaining good agreement as well.

Therefore, the true yield of single-ion and ion-pair production can be obtained by correcting the measured yield to the detection and transmission efficiencies, i.e., for the single-ion OH^+ production the true yield Y^{true} can be written accordingly:

$$Y^{\text{true}}(OH^+) = \frac{Y^{\text{meas}}(OH^+)}{\bar{\epsilon}} - \left(\frac{\bar{\epsilon}(1-\bar{\epsilon})}{\bar{\epsilon}}\right) \times Y^{\text{true}}(H^+ + OH^+), \quad (1)$$

where Y^{true} are the true yields of single-ion OH^+ production and $H^+ + OH^+$ pair-ion production. The latter is given by

$$Y^{\text{true}}(H^+ + OH^+) = \frac{Y^{\text{meas}}(H^+ + OH^+)}{\bar{\epsilon}^2}. \quad (2)$$

The probability of detecting only the single ion OH^+ from the $H^+ + OH^+$ ion pair is given by $\bar{\epsilon}(1-\bar{\epsilon})$, which takes into account the detection of a single ion OH^+ ($\bar{\epsilon}$) constrained by the lack of detection of the transmitted fast H^+ ion $(1-\bar{\epsilon})$.

A similar set of equations can be written for the O^+ single-ion yield and $H^+ + O^+$ ion-pair yield. For the production of H_2O^+ and H^+ ions the true yields are written as

$$Y^{\text{true}}(H_2O^+) = \frac{Y^{\text{meas}}(H_2O^+)}{\bar{\epsilon}} \quad (3)$$

and

$$Y^{\text{true}}(H^+) = \left(\frac{Y^{\text{meas}}(H^+)}{\bar{\epsilon}}\right) - \left(\frac{1-\bar{\epsilon}}{\bar{\epsilon}^2}\right) \times \left(Y^{\text{meas}}(H^+ + OH^+) + \sum_q Y_q^{\text{meas}}(H^+ + O^{q+})\right). \quad (4)$$

We have found $\epsilon = 0.10 \pm 0.01$. The true yield was corrected and the cross section waas obtained by normalizing the total positive-ion production yield for the cross section σ^+ of Rudd *et al.* [33].

III. RESULTS AND DISCUSSION

After collision with a proton projectile, the water molecule can have electrons removed from any molecular orbital, which leads to final states where the molecule can be dissociated. Ionization leading to the removal of two electrons can originate from the removal of two sequential electrons (TS2) or the removal of a single electron followed by an Auger-like deexcitation leading to a second electron emission. Those mechanisms compete in importance and, within the first-order Born approximation, they should have different energy dependences. For proton impact, the mechanism should have an energy dependence of $\sim \ln(E)/E$ for ionization occurring from a single-vacancy process and $\sim 1/E^2$ for ionization occurring from sequential double vacancies.

Figure 1 shows the measured branching ratios for proton impact (closed symbols) of double-ionization channels $H^+ + O^+$ [Fig. 1(a)] and $H^+ + OH^+$ [Fig. 1(c)] obtained via double-hit measurements and single-ionization channels $O^+ +$ neutral [Fig. 1(b)] and $OH^+ +$ neutral [Fig. 1(d)] obtained via single-hit measurements. All ratios are with respect to the

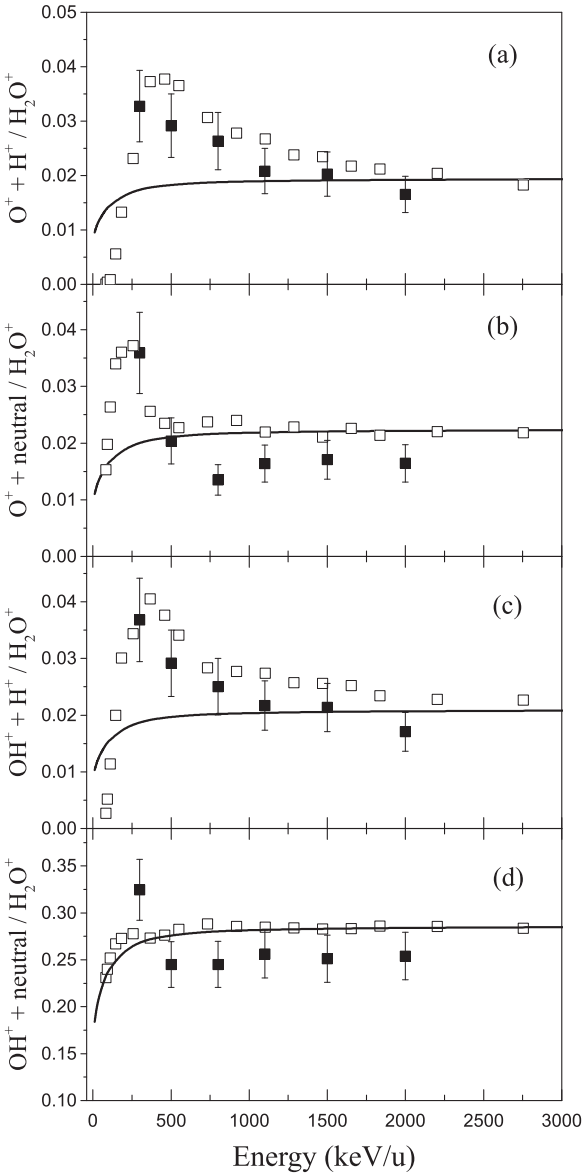

FIG. 1. Ratios with respect to the H_2O^+ production for double-ionization channels (a) $H^+ + OH^+$ and (b) $H^+ + O^+$ and single-ionization channel (c) O^+ + neutral: proton impact (this work), closed symbols; electron impact (Refs. [18,19]); open symbols; and our calculation for proton impact, solid line.

single ionization without a dissociation channel (H_2O^+). For completeness, the results are also compared to the ratios of equivelocity electron impact from Ref. [18] (open symbols). The branching ratios agree in magnitude for both projectiles and in the asymptotic limit of higher velocities the branching ratios tend to be constant for the single-ionization and the double-ionization ratios.

A semiempirical calculation was used to describe the proton- (our work) and electron- (Refs. [18,19]) impact ionization cross section σ_{nl} (in units of Mb) for the water molecule. In this model, the ionization cross section of protons or electrons follows the scaling law [25,26]

$$\frac{\sigma_{nl} I_{nl}^2}{Z_{nl}\delta_{nl}} = F\left(\frac{E/M}{I_{nl}}\right), \quad (5)$$

where

$$F(x) = \frac{A\ln(1+Bx)}{x} - \frac{AB}{(1+cx)^4}, \quad (6)$$

with $A = 5000$, $B = 0.1$, $C = 0.0125$ corresponding to the $2a_1$ molecular orbital, E/M in keV/u for the proton case, and the ionization potentials I_{nl} given in rydbergs. The label nl represents a particular molecular orbital. For the electron case, two changes in the above equations were introduced in Ref. [26] as an ansatz to take into account the ionization threshold as well as the change in the shape of the cross section for energies (in eV) below the maximum: $x = 1.836E/I_{nl} - 24.97$. Thus, at the threshold energy $E = 13.6I_{nl}$ Ry, $x = 0$, and $F(x) = 0$.

The fragment species cross sections σ_i is obtained from the cross section σ_j for each valence shell j contributing to its formation through an appropriate percentage f_{ij} (fragmentation matrix) such that $\sigma_i = \sum_{j=1}^{n} f_{ij}\sigma_j$ with the constraint $\sum_i^n f_{ij} = 1$, where n is the number of fragment species considered [34]. All parameters were adjusted to give better general agreement with the measured total ionization cross sections of Ref. [33].

As can be seen in Figs. 1(a)–1(d), all ratios from both proton and electron impact show asymptotically a constant value trend. Based on this behavior, the semiempirical calculation for proton impact (solid line) is adjusted to match the asymptotic experimental branching ratios by setting the probabilities fractions f_{ij} as free parameters in the calculation. These f_{ij} are associated with the water molecular orbitals $1b_1$, $3a_1$, $1b_2$, and $2a_1$ (prompt and Auger) with ionization potentials of 12.61, 15.57, 19.83, and 36.88 eV, respectively. The values obtained for the fractions f_{ij} are summarized in Table I. Except for the orbital $2a_1$, all other fractions are the same as those presented in Ref. [7]. The values associated with the $2a_1$ orbital are slightly different from those reported in [35], where the contributions related to the Auger decay of the $2a_1$ orbital were not considered explicitly. The former values have been used in some calculations such as work of Murakami *et al.* [36] and the classical approach for the ion fragment production by Illescas *et al.* [37].

The $H^+ + H^+ + O$ channel was not measured in this experiment. For the velocity region dominated by Auger decay there are no previous measurements for this fraction ($f_{H^+ + H^+, 2a_1}$). In Table I it was assumed that $f_{H^+ + H^+, 2a_1} = 0$. For $f_{H^+ + H^+, 2a_1} \neq 0$ [38] the fraction of H^+ corresponding to $2a_1$ orbital would be given by $f_{H^+, 2a_1} = 0.58 - f_{H^+ + H^+, 2a_1}$, without other changes to the values in Table I.

Separation in the molecular fragmentation pathways is important in order to obtain quantitatively the contribution from prompt ionization (single and double) and ionization occurring from an Auger-like decay. In the case of water, for vacancies occurring in the $2a_1$ inner valence molecular orbital, the Auger-like deexcitation channel leading to a double ionization occurs in competition with a prompt fragmentation leading to a singly ionized fragment. From the fitting procedure in the semiempirical calculation shown in Fig. 1 (solid line), the contribution of an Auger-like postcollisional deexcitation from the $2a_1$ valence orbital could be evaluated. We have found that it accounts for at least 27% of the $2a_1$ contribution to the total molecular ionization: 14% and 13% for $H^+ + OH^+$ and $H^+ + O^+$, respectively (see Table I).

TABLE I. Fractions f_{ij}.

Channel	$1b1$	$3a1$	$1b2$	$2a_1$ (prompt)	$2a_1$ (Auger)
H_2O^+	1	1	0.08		
$OH^+ + H$			0.7		
$OH^+ + H^+$					0.14
$O^+ + H$				0.15	
$O^+ + H^+$					0.13
H^+			0.22	0.58	

Specifically, the cross sections of the fragments associated with simple ionization of orbital $2a_1$, under the assumptions described in the preceding paragraph, can be written as

$$\sigma(H^+ + O^+) = 0.13\sigma(2a_1),$$
$$\sigma(H^+ + OH^+) = 0.14\sigma(2a_1),$$
$$\sigma(O^+ + 2H(H_2)) = 0.15\sigma(2a_1),$$
$$\sigma(H^+ + OH) = 0.22\sigma(1b2) + 0.58\sigma(2a_1),$$

where the first two equations correspond to Auger decay and the last two to prompt decay. These two decay modes compete and should occur in the same time scale. Extrapolating the

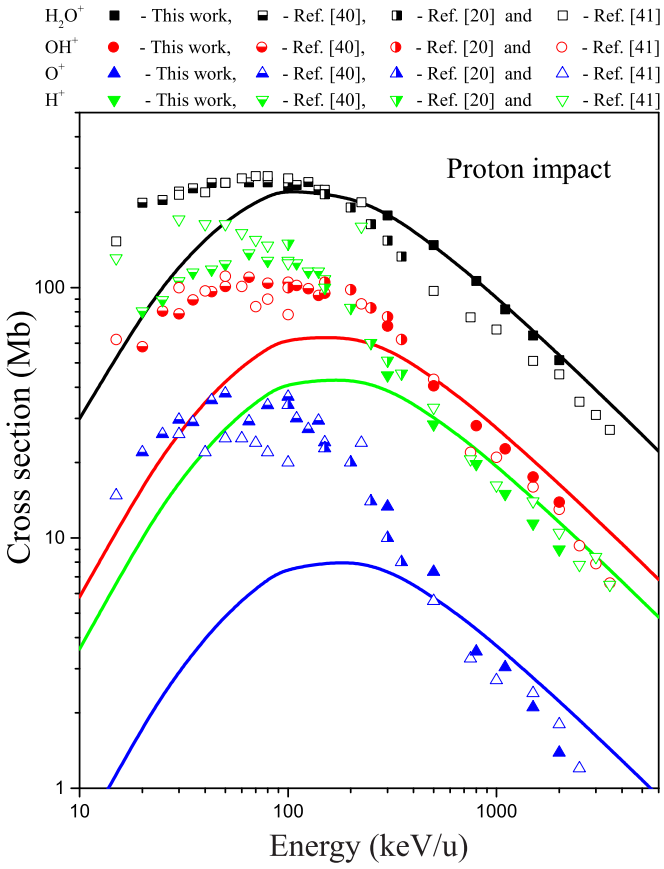

FIG. 2. (Color online) Proton-impact cross sections leading to the formation of the target product channels H_2O^+ (black symbols), OH^+ (red symbols), O^+ (blue symbols), and H^+ (green symbols). The compiled data refer to this work, closed symbols; Ref. [41], open symbols; Ref. [20], right closed symbols; and Ref. [40], bottom closed symbols. The present calculations are represented by the solid lines.

Auger widths given by Campbell and Papp [39] to the oxygen $2s$ shell, an estimate of ~ 9.2 fs can be assigned to the Auger decay time of the $2a_1$ orbital. Because of the larger contribution from the prompt decay to fragmentation from the $2a_1$ orbital, this decay mode should be faster compared to Auger decay, although within the same time scale.

Figure 2 shows a comparison of our experimental results and our model calculation with the proton-impact data available in the literature for the energy range of 10–3500 keV/u [20,40,41]. Good agreement between the available experimental data is observed. The calculation also shows overall good agreement for the production of H_2O^+, OH^+, O^+, and H^+ cross sections at higher velocities. This agreement is an indication that processes linked to single primary vacancy production prevails (i.e., single ionization or Auger decay double ionization).

Figure 3 shows the same comparison of Fig. 2 with the model parameters extended to the electron-impact case. The model is compared to a compilation of experimental electron-impact cross-section data leading to the formation of the target product channels H_2O^+, OH^+, O^+, and H^+ from Refs. [18,19,42–44] in the energy-mass range of 15–5000 keV/u. It is important to note that overall good agreement is achieved with the calculation from the present work despite the considerable dispersion among the data available in the literature.

Comparing the results shown in Figs. 2 and 3, we can promptly verify that for the proton case, for energies below ≈400 keV/u, there is a clear disagreement between the experimental data and the model calculation for the total production of H^+, OH^+, and O^+, being more prominent for the O^+ case. In fact, theses products can be generated by either dissociation after single ionization or double ionization of the former molecule. Therefore, the disagreement with the model below that energy can be considered as an indication that in the lower-energy range the direct process (TS2) takes over the Auger decay in the double-ionization mechanism. Indeed, calculations including single, double, and triple ionization by Murakami *et al.* [36,45] for proton impact show good agreement with the fragmentation data for energies above the cross-section maxima. It is interesting to note that for electrons this behavior is not seen so clearly and there is good agreement within the entire energy range investigated. In fact, this occurs because electrons carry lower momentum than protons with the same velocity and as the energy decreases the transferred momentum is not sufficient to produce two-sequential-vacancy ionization (TS2).

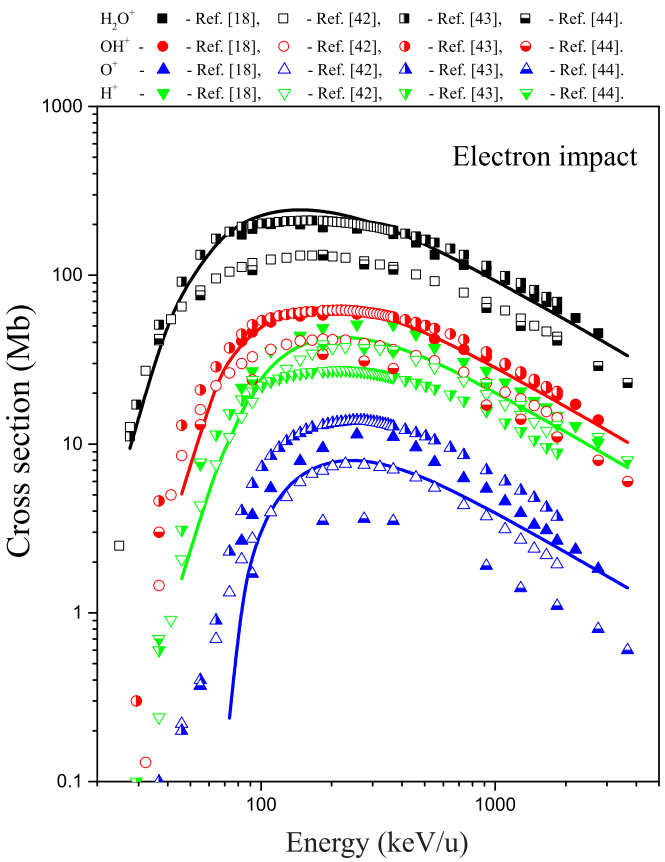

FIG. 3. (Color online) Electron-impact cross sections leading to the formation of the target product channels H_2O^+, OH^+, O^+, and H^+. The compiled data refer to Ref. [18], closed symbols; Ref. [42], open symbols; Ref. [43], right closed symbols; and Ref. [44], bottom closed symbols. The present calculations are represented by the solid lines.

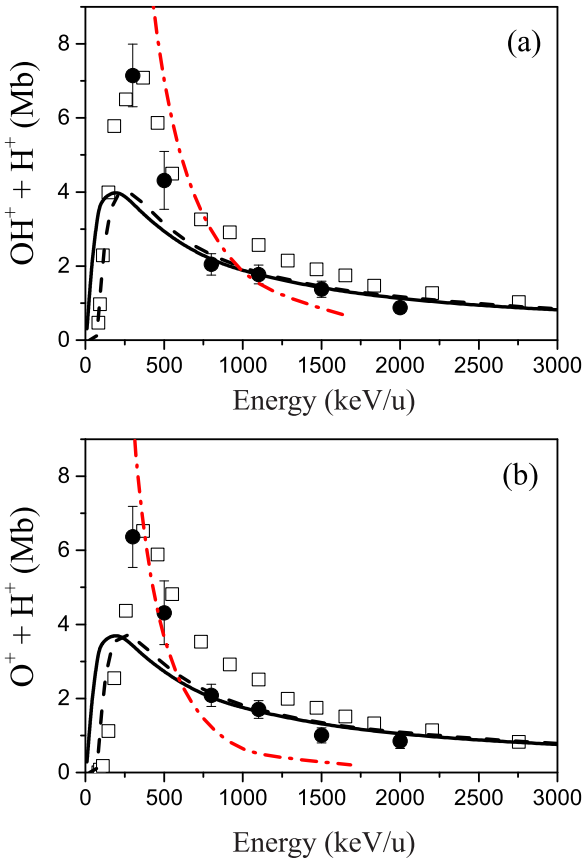

FIG. 4. (Color online) Cross sections for double-ionization channels (a) $H^+ + OH^+$ and (b) $H^+ + O^+$: proton impact (this work), closed circles; electron impact (Refs. [18,19]), open squares; our calculation for proton impact; solid line; our calculation for electron impact, dashed line; and quantum-mechanical calculation of Ref. [36] for proton impact, red dot-dashed line.

TABLE II. Double-ionization cross sections (Mb).

Energy (keV)	$H^+ + OH^+$	$H^+ + OH^+$
300	7.2 ± 0.9	6.4 ± 0.8
500	4.3 ± 0.8	4.3 ± 0.5
800	2.0 ± 0.3	2.1 ± 0.3
1100	1.8 ± 0.3	1.7 ± 0.2
1500	1.4 ± 0.2	1.0 ± 0.2
2000	0.88 ± 0.15	0.85 ± 0.18

Examining the double-ionization cross sections, the relative contribution from TS2 and Auger-like decay can be discussed in more detail. Figure 4 shows cross sections for double ionization of water by protons (closed symbols) and electrons (open symbols) from Ref. [18] as well as our semiempirical calculation (black solid line and black dashed line for proton and electron impact, respectively). Our measured cross sections are summarized in Table II.

The quantum-mechanical calculation of Murakami *et al.* [36] for proton impact is also included in the figure (red dot-dashed line). As can be seen, for both channels $H^+ + OH^+$ [Fig. 4(a)] and $H^+ + O^+$ [Fig. 4(b)], there is a similar behavior for proton- and electron-impact data over the energy range studied this work. Its is important to note that the theory of Murakami *et al.* theory takes only projectile-induced mechanisms into account to describe the double ionization, while our model uses only Auger-like decay to describe it. As can be seen in Fig. 4, the cross sections are well described by our model at higher energies ($\sim$750 keV/u), indicating that above this energy the double-ionization mechanism is dominated by Auger decay. For energies below 750 keV/u, on the other hand, the cross section is in better agreement with the calculation of Murakami *et al.* [36,45], a clear indication that the TS2-like process becomes dominant.

IV. CONCLUSION

Double-ionization cross sections of a water molecule leading to $H^+ + OH^+$ and $H^+ + O^+$ fragmentation channels were measured for proton impact in the energy range of 300–2000 keV/u, using a double-hit measurement procedure. From the single-hit measurement the prompt single-ionization channel $O^+ + 2H$ (H_2) was also obtained. With the aid of a semiempirical model, it was possible from our measurements to ascribe quantitatively the contribution from the Auger-like mechanism and from the prompt fragmentation to the decay of a vacancy occurring in the $2a_1$ molecular orbital. It was found that the main contribution accounts for the prompt fragmentation resulting in the ejection of only one charged ion.

Furthermore, it was found that for lower energies the TS2 process is the main mechanism leading to double ionization of the water molecule. For higher energies, on the other hand, single vacancy followed by an Auger-like deexcitation takes over the TS2 process and becomes the main contribution to the double-ionization cross section and accounts for roughly $\sim$4% of the total ionization.

Finally, the results discussed in this work lead to more restrictive tests of the theory since they allow one to separate quantitatively the mechanisms that contribute to the double ionization. In particular, the limits of a perturbative-type description of double ionization of water, such as those presented by Oubaziz *et al.* [46] for electron impact, can be advantageously verified by proton impact.

ACKNOWLEDGMENTS

The authors gratefully acknowledge financial support from Fundação Carlos Chagas Filho de Amparo à Pesquisa do Estado do Rio de Janeiro and Conselho Nacional de Desenvolvimento Científico e Tecnológico (Brazil).

[1] A. Brahme, Int. J. Radiat. Oncol. Biol. Phys. **58**, 603 (2004).
[2] E. J. Hall, *Radiobiology for the Radiologist*, 5th ed. (Lippincott, Williams, & Wilkins, Philadelphia, 2000).
[3] H. Chang, W. Oehrl, P. Elsner, and J. J. Thiele, Free Radical Res. **37**, 655 (2003).
[4] D. T. Hall *et al.*, Nature **373**, 677 (1995).
[5] B. C. Garrett *et al.*, Chem. Rev. **105**, 355 (2005).
[6] J. Suarez, L. Méndes, and J. Rabadán, J. Chem. Phys. Lett. **6**, 72 (2015).
[7] E. C. Montenegro, J. Phys.: Conf. Ser. **194**, 012049 (2009).
[8] J. H. McGuire, Phys. Rev. Lett. **49**, 1153 (1982).
[9] B. El Marji *et al.*, J. Phys. B **30**, 3677 (1997).
[10] S. D. Lopez, S. Otranto, and C. R. Garibotti, Phys. Rev. A **89**, 062709 (2014).
[11] C. A. Tachino, M. E. Galassi, and R. D. Rivarola, Phys. Rev. A **80**, 014701 (2009).
[12] C. C. Montanari, J. E. Miraglia, W. Wolff, H. Luna, A. C. F. Santos, and E. C. Montenegro, J. Phys.: Conf. Ser. **388**, 012036 (2012).
[13] C. C. Montanari, E. C. Montenegro, and J. E. Miraglia, J. Phys. B **43**, 165201 (2010).
[14] C. D. Archubi, C. C. Montanari, and J. E. Miraglia, J. Phys. B **40**, 943 (2007).
[15] T. Spranger and T. Kirchner, J. Phys. B **37**, 4159 (2004).
[16] E. G. Cavalcanti, G. M. Sigaud, E. C. Montenegro, M. M. SantAnna, and H. Schmidt-Böcking, J. Phys. B **35**, 3937 (2002).
[17] E. G. Cavalcanti, G. M. Sigaud, E. C. Montenegro, and H. Schmidt-Böcking, J. Phys. B **36**, 3087 (2003).
[18] E. C. Montenegro, S. W. J. Scully, J. A. Wyer, V. Senthil, and M. B. Shah, J. Electron. Spectrosc. Relat. Phenom. **155**, 81 (2007).
[19] S. W. J. Scully, J. A. Wyer, V. Senthil, M. B. Shah, and E. C. Montenegro, Phys. Rev. A **73**, 040701R (2006).
[20] U. Werner, K. Beckord, J. Becker, and H. O. Lutz, Phys. Rev. Lett. **74**, 1962 (1995).
[21] F. Alvarado, R. Hoektra, and T. Schlathölten, J. Phys. B **38**, 4085 (2005).
[22] I. Ben-Itzhak *et al.*, Nucl. Instrum. Methods Phys. Res. Sect. B **233**, 284 (2005).
[23] Z. D. Pesić, R. Hellhammer, B. Sulik, and N. Stolterfoht, J. Phys. B **42**, 235202 (2009).

[24] S. Martin, L. Chen, R. Brédy, J. Bernard, and A. Cassimi, J. Chem. Phys. **142**, 094306 (2015).
[25] E. C. Montenegro, G. M. Sigaud, and R. D. DuBois, Phys. Rev. A **87**, 012706 (2013).
[26] W. Wolff, H. Luna, L. Sigaud, A. C. Tavares, and E. C. Montenegro, J. Chem. Phys. **140**, 064309 (2014).
[27] J. Meesungnoen and J.-P. Jay-Gerin, Radiat. Res. **171**, 379 (2009).
[28] B. Gervais, M. Beuve, G. H. Olivera, M. E. Galassi, and R. D. Rivarola, Chem. Phys. Lett. **410**, 330 (2005).
[29] C. Champion, Phys. Med. Biol. **55**, 11 (2010).
[30] D. Oubaziz, C. Champion, and H. Aouchiche, Phys. Rev. A **88**, 042709 (2013).
[31] W. Wolff, I. J. de Souza, A. C. Tavares, G. F. S. de Oliveira, and H. Luna, Rev. Sci. Instrum. **83**, 123107 (2012).
[32] I. Ben-Itzhak, S. G. Ginther, and K. D. Carnes, Phys. Rev. A **47**, 2827 (1993).
[33] M. E. Rudd, T. V. Goffe, R. D. DuBois, and L. H. Toburen, Phys. Rev. A **31**, 492 (1985).
[34] E. C. Montenegro, L. Sigaud, W. Wolff, H. Luna, and N. Ferreira, Phys. Proc. **66**, 39 (2015).
[35] K. H. Tan, C. E. Brion, P. E. Van der Leeuw, and J. Van der Wiel, Chem. Phys. **29**, 299 (1978).
[36] M. Murakami, T. Kirchner, M. Horbatsch, and H. J. Ludde, Phys. Rev. A **85**, 052704 (2012).
[37] C. Illescas, L. F. Errea, L. Mendez, B. Pons, I. Rabadán, and A. Riera, Phys. Rev. A **83**, 052704 (2011).
[38] H. B. Pedersen *et al.*, Phys. Rev. A **87**, 013402 (2013).
[39] J. L. Campbell and T. Papp, At. Data Nucl. Data Tables **77**, 1 (2001).
[40] F. Gobet, S. Eden, B. Coupier, J. Tabet, B. Farizon, M. Farizon, M. J. Gaillard, M. Carreé, S. Ouaskit, T. D. Mark, and P. Scheier, Phys. Rev. A **70**, 062716 (2004).
[41] H. Luna, A. L. F. de Barros, J. A. Wyer, S. W. J. Scully, J. Lecointre, P. M. Y. Garcia, G. M. Sigaud, A. C. F. Santos, V. Senthil, M. B. Shah, C. J. Latimer, and E. C. Montenegro, Phys. Rev. A **75**, 042711 (2007).
[42] B. G. Lindsay and M. A. Mangan, in *Photon and Electron Interactions with Atoms, Molecules and Ions*, edited by Y. Itikawa, Landolt-Börnstein, Group I, Vol. 17, Pt. C (Springer, New York, 2003).
[43] M. V. V. S. Rao, I. Iga, and S. K. Srivastava, J. Geophys. Res. **100**, 26421 (1995).
[44] J. Schutten, F. J. deHeer, H. R. Moustafa, A. J. H. Boerboom, and J. Kistemaker, J. Chem. Phys. **44**, 3924 (1966).
[45] M. Murakami, T. Kirchner, M. Horbatsch, and H. J. Ludde, Phys. Rev. A **85**, 052713 (2012).
[46] D. Oubaziz, M. A. Quinto, and C. Champion, Phys. Rev. A **91**, 022703 (2015).